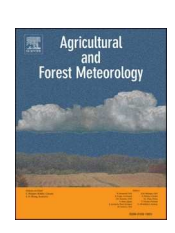
ELSEVIER

Contents lists available at ScienceDirect

### Agricultural and Forest Meteorology

journal homepage: www.elsevier.com/locate/agrformet





# Probing the interplay of biophysical constraints and photosynthesis to model tree growth

Antoine Cabon <sup>a,\*</sup>, Aitor Ameztegui <sup>b,c</sup>, William R.L. Anderegg <sup>d,e</sup>, Jordi Martínez-Vilalta <sup>f,8</sup>, Miquel De Cáceres <sup>f</sup>

- <sup>a</sup> Swiss Federal Institute for Forest, Snow and Landscape Research WSL, Birmensdorf, Switzerland
- <sup>b</sup> Department of Agricultural and Forest Sciences and Engineering, Universitat de Lleida, Lleida, Catalonia, Spain
- <sup>c</sup> Joint Research Unit CTFC-Agrotecnio-CERCA, Solsona, Catalonia, Spain
- <sup>d</sup> School of Biological Sciences, University of Utah, Salt Lake City, UT, USA
- e Wilkes Center for Climate Science and Policy, University of Utah, Salt Lake City, UT, USA
- f CREAF, Bellaterra (Cerdanyola del Vallès), Catalonia E08193, Spain
- g Autonomous University of Barcelona, Bellaterra (Cerdanyola del Vallès), Catalonia E08193, Spain

#### ARTICLE INFO

# Keywords: Photosynthesis Biophysical Source-sink interactions Lockhart equation Tree growth Modelling

#### ABSTRACT

Tree growth is a key uncertainty in projections of forest productivity and the global carbon cycle. While global vegetation models commonly represent tree growth as a carbon assimilation (source)-driven process, accumulating evidence points toward widespread non-photosynthetic (sink) limitations. Notably, growth biophysical potential, defined as the upper-limit to tree growth imposed by temperature and turgor constraints on cell division, has been suggested to be a potent driver of observed decoupling between tree growth and photosynthesis. Understanding the interplay between biophysical potential and photosynthesis and how to accommodate it parsimoniously in models remains a challenge.

Here, we use a soil-plant-atmosphere continuum model together with a regional network of forest structure and annual, radial tree growth observations extending over three decades to simulate tree photosynthesis and biophysical potential along an aridity gradient and across five tree species in NE Spain. We then apply a linear modelling framework to quantify the relative importance of photosynthesis, biophysical potential and their interactions to predict annual tree growth along the aridity gradient.

Overall similar relative importance of photosynthesis and biophysical potential was underlain by strong variations with climate, photosynthesis being more relevant at wet sites and biophysical potential at dry sites. Observed spatial and temporal trends further suggested that tree growth is primarily limited by biophysical potential under dry conditions and that disregarding it could lead to underestimating tree growth decline with increased aridity under climate change.

Our results support the idea that biophysical potential is an important component of sink limitations to tree radial growth. Its representation in vegetation models could accommodate spatially and temporally dynamic source-sink limitations on tree growth.

#### 1. Introduction

Forests provide numerous ecosystem services and play a key role in global carbon cycling by storing a fourth of anthropogenic  $CO_2$  emissions (Pan et al., 2011; Friedlingstein et al., 2022). Forests' ability to store carbon (C) is determinant to future climate trajectories (Bonan, 2008), but also directly depends upon climate. Acknowledging this important feedback, future climate projections are typically simulated

using Earth system models with a land sub-model that often includes a Dynamic Global Vegetation Model (DGVM) (Fisher et al., 2018). DGVMs aim to represent major vegetation processes, including vegetation photosynthesis, growth and demography, that in turn determine land C, water, and nutrient cycles (Bonan, 2008; Quillet et al., 2010). For a given climate forcing, projections of C uptake by DGVMs hence fundamentally depends on their capacity to accurately represent these processes (Pappas et al., 2013). Model uncertainty imputable to model

E-mail address: antoine.cabon@wsl.ch (A. Cabon).

<sup>\*</sup> Corresponding author.

structure and parameterization can be quantified based on model ensembles, sensitivity analyses and error propagation approaches (Smith et al., 2009; Collins et al., 2012). From such approaches, C residence time in forest ecosystems is estimated to rank among the largest contributors to model uncertainty of global carbon balance (Friend et al., 2014; Pugh et al., 2020). Further uncertainty may arise from process conceptualization not yet reflected in existing models. Most DGVMs represent allocation to woody growth as a fraction of net primary production, based on an allocation coefficient approach (C source limitation) (Franklin et al., 2012; Merganičová et al., 2019). However, increasing evidence suggests that direct environmental control of cambial activity (C sink limitation) may substantially limit C allocation to woody growth, leading to a decoupling of growth and carbon assimilation and casting further uncertainty on C residence time (Fatichi et al., 2014; Körner, 2015; Cabon et al., 2022).

Sink limitations to tree growth may occur as a result of cambial phenology, nutrient availability, or biophysical constraints of water potential and temperature on cambial cell division and expansion rates (Körner, 2015). Cambial activity is expected to be more sensitive than photosynthesis to low water availability and temperature, as cell expansion and division are strongly limited at water potentials under ~ -1MPa and temperatures below ~5°C, while photosynthesis is still operating (Rossi et al., 2008; Muller et al., 2011). Hence, tree growth is expected to be more sink-limited in arid and cold environments, which can be illustrated by an accumulation of non-structural carbohydrates under such conditions (Woodruff and Meinzer, 2011; Hoch and Körner, 2012; Piper et al., 2017).

Acknowledging the importance of sink limitations on tree growth, several approaches have been proposed to integrate source and sink limitations within existing frameworks (Guillemot et al., 2015, 2017; Fatichi et al., 2019; Friend et al., 2019). However, it is not yet clear how photosynthate availability influences wood formation, and what model structure would thus be best suited to describe source-sink relations in a robust and parsimonious way. Models should notably match observations of the relative importance of source and sink drivers in explaining tree growth, as well as its variation across space and time. Source-sink relative importance likely depends on species and environmental conditions (Guillemot et al., 2015; Cabon et al., 2022), but identifying general trends is complicated by large source-sink covariation (Körner, 2015). A linear modelling framework can provide a first step toward better understanding of source-sink relative importance and its variations (i.e., multiplicative and/or additive interactions) whilst accounting for source-sink covariation.

Turgor-driven tree growth has been proposed as a fundamental mechanism to explain sink limitations to tree growth. A large family of turgor-driven growth models allow highly mechanistic simulations of tree growth at fine scales (Steppe et al., 2006; Hölttä et al., 2010; Coussement et al., 2018; Peters et al., 2021; Potkay et al., 2022; Potkay and Feng, 2023). These models represent a promising avenue to integrate source and sink activities but require upscaling and simplification in order to be implemented within DGVMs (Fatichi et al., 2019; Cabon and Anderegg, 2022). In essence, turgor-driven models are based on the consideration that cambial activity notably relies on cell turgor, which provides the physical force for cell expansion and can be described using a linear equation (Lockhart, 1965). Cell turgor in turn depends on cell water potential, which thus strongly controls cell expansion in the cambium (Hsiao, 1973; Muller et al., 2011). As cambial cells need to double their volume during mitosis, Lockhart's linear equation for cell expansion can also be applied to describe the biophysical effect of turgor and water potential on cell division rate and tree growth (Cabon et al., 2020b; Peters et al., 2021). Similarly, temperature may directly limit cell expansion and division through its effect on enzymatic activity, which can be described based on thermodynamics principles (Parent et al., 2010; Parent and Tardieu, 2012). Such effect can be accommodated in Lockhart's equation as changes in cell wall extensibility (Pietruszka et al., 2007; Cabon et al., 2020b). The turgor-driven growth framework

hence allows to represent the biophysical limitations of water potential and temperature on tree growth. This framework could further accommodate the effect of C availability on wood formation (Hölttä et al., 2010; Potkay et al., 2022). For example, monitoring of carbohydrate concentration during xylogenesis suggests that C availability in the cambium partially controls the number of cells undergoing division and differentiation during wood formation (Deslauriers et al., 2009, 2016). Girdling experiments further show that increased C concentration may overcome the effect of drought on wood formation, arguably by allowing the cambium to develop lower osmotic potential (Winkler and Oberhuber, 2017). Likewise temperature, the effect of carbohydrate availability on tree growth could therefore be modelled through its effect on Lockhart's equation parameters, e.g., by modifying cell wall extensibility or the osmotic potential (Hölttä et al., 2010; Cartenì et al., 2018; Potkay et al., 2022). Lockhart's biophysical equation hence appears as a good candidate for mechanistic integration of source and sink limitations to tree radial growth.

Here we use tree growth, physiological and strand structure observations across five species along a climate gradient in NE Spain, together with a soil-plant-atmosphere model, to test the usefulness of explicitly simulating the constraints exerted by temperature and water potential that reduce the biophysical potential for growth. More specifically, we aim to (1) unravel the sensitivity of simulated photosynthesis and biophysical potential to shared drivers and their covariation under across an aridity gradient, (2) assess the unique and joint ability of photosynthesis and biophysical potential to explain the observed variation in tree radial growth and (3) better understand how environmental conditions may shape the relative importance of source and sink limitations on tree growth and implications in the context of modelling.

#### 2. Material and methods

#### 2.1. Study area and tree growth observations

Five species were selected among the most common forest trees in Catalonia (NE Spain): Pinus halepensis, P. nigra, P. sylvestris, Quercus pubescens and Fagus sylvatica (Fig. 1). Fifteen National Forest Inventory plots dominated by each of the previous species were selected to represent the local climatic range of each species in terms of water availability. Overall, the 75 plots selected (15 plots x 5 species) spanned the whole forested area of Catalonia and captured a large climatic gradient ( $\sim 10^{\circ}$ C in mean annual temperature and  $\sim 800$ mm in annual precipitation differential). More details on the experimental design and field sampling protocols can be found in Serra-Maluquer et al. (2018), Rosas et al. (2019), and González de Andrés et al. (2021).

In order to estimate tree radial growth, one wood core per tree was sampled at breast height in 2015, on five adult trees (diameter at breast height > 12.5cm) per plot, within 25 m of the plot center. Cores of 5mm diameter were extracted using an increment borer. In the laboratory cores were mounted, dried and polished. Cores were then scanned at 1200 dpi resolution and tree-ring width was measured and cross-dated following standard dendrochronology methodology (Cook and Kairiukstis, 2013), using CooRecorder and cDendro (Cybis Elektronik) (Serra-Maluquer et al., 2018). Individual ring width series were used to infer past tree diameter at breast height from measured tree diameter in 2015. Ring width series were then corrected for the effect of tree size based on species-level empirical equations, where tree radial growth is modelled as a log normal function of initial tree diameter (Gómez-Aparicio et al., 2011). These equations were calibrated at the national level using national forest inventory data while controlling for the effects of climate and competition on tree growth, hence allowing to capture the effect of tree size on tree radial growth, independently of climate and stand structure. Size-corrected tree radial growth was calculated as the ratio between raw ring width and expected tree growth modelled from diameter. Individual ring width series covering the period 1990-2015 were finally scaled (z-score) and aggregated at the

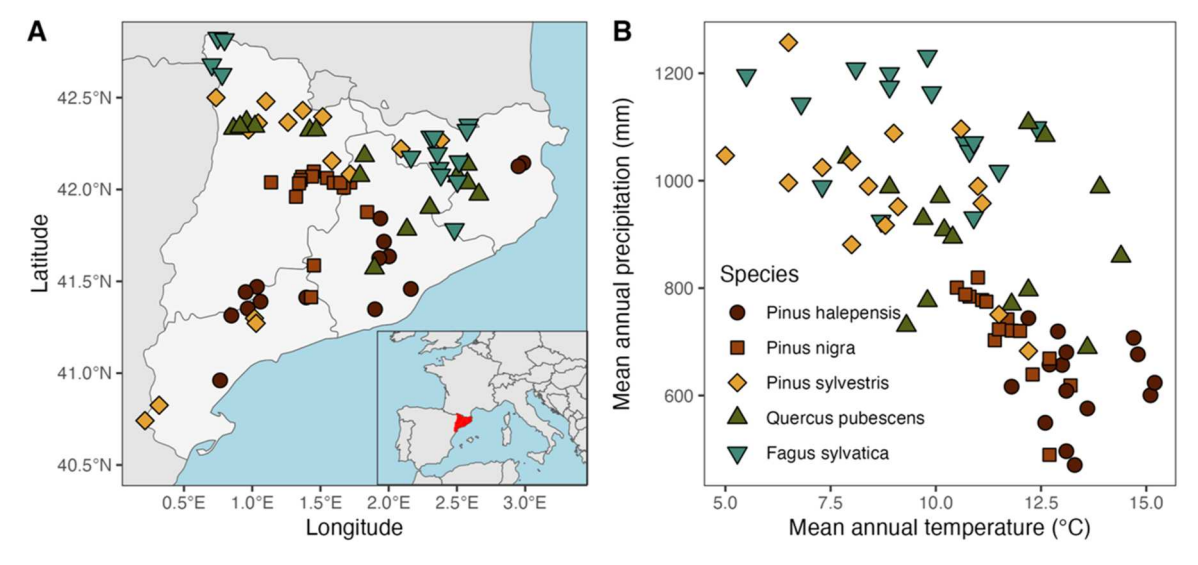


Fig. 1. (A) Geographic and (B) climatic data distribution. Tree-ring data were collected at 15 plots across the distribution of five common tree species in Catalonia (NE Spain), spanning a ~10°C temperature and ~800mm precipitation gradient.

plot scale (Fig. 2). Plot-level tree-ring width series were later used to fit statistical tree radial growth models and test the relative importance of source and sink processes in explaining tree radial growth.

#### 2.2. Soil-plant-atmosphere continuum model

We used the soil-plant-atmosphere continuum model from the R

package medfate, which has been extensively applied and tested in the study area (De Cáceres et al., 2015, 2021; Cabon et al., 2018), in order to simulate tree C assimilation as well as the turgor component of the biophysical potential of tree growth. medfate uses climate forcing together with a representation of soil physical properties, species hydraulic traits and stand structure, including tree and shrub leaf area and root distribution, to simulate water,  $\mathrm{CO}_2$  and energy balances at the

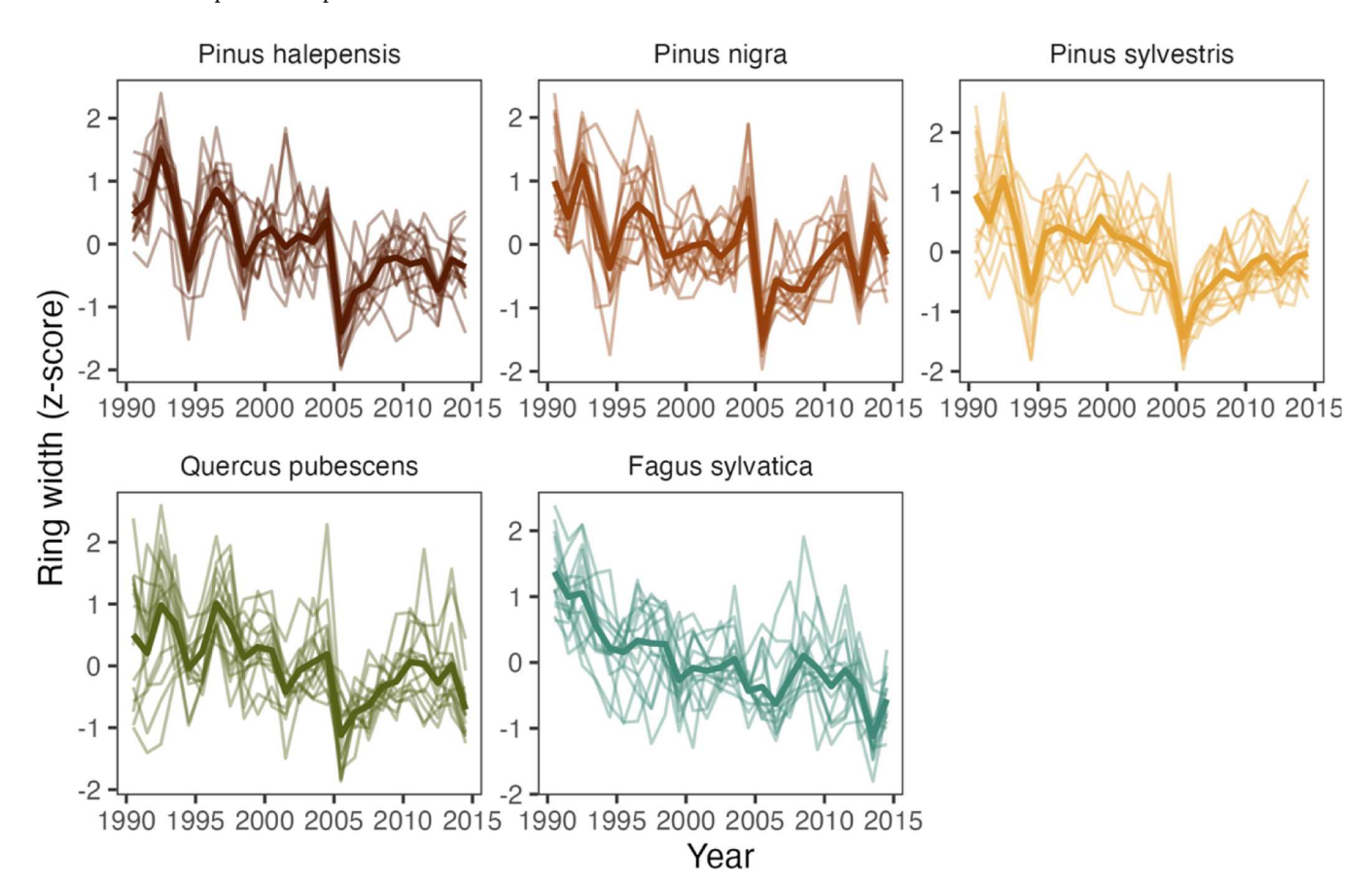


Fig. 2. Observed tree radial growth. Ring width data were corrected for the effect of tree size and scaled (z-score). Thin lines represent plot averages and thick lines are species averages. Statistics on plot-level chronologies can be found in Table S1. Gymnosperm (upper row) and angiosperm species (lower row) are ordered according to their distribution from xeric (left) to mesic (right).

cohort level. Cohorts were defined here as all conspecific individuals, and we thus ran the model at each plot to simulate stem water potential and tree photosynthesis at the sub-daily scale and at the species level. Non-physiological variables are simulated at the plot level. Note that whereas the latest medfate version (De Cáceres et al., 2023) includes a plant growth module, it was not used in the present study. Soil water balance is essentially calculated as the difference between water influx and outflux, the main fluxes being precipitation and plant transpiration. Transpiration is a function of soil-to-leaf hydraulic conductance and the water potential gradient imposed by soil water potential, atmospheric conditions and stomatal conductance (De Cáceres et al., 2021). Stomatal conductance is simulated based on optimality theory of stomatal control, where stomata balance carbon gain and risk of hydraulic failure (Sperry et al., 2017). Tree water potential at breast height can in turn be calculated from the transpiration rate, hydraulic conductance and soil water potential. The transpiration rate and the leaf energy balance further allow to simulate leaf CO2 concentration and gross photosynthesis from carboxylation- and electron transport-limited photosynthesis, following Collatz et al. (1991) and Medlyn et al. (2002). Net photosynthesis is finally calculated by discounting leaf respiration, which is a function of the carboxylation rate. For more details on the model the reader is referred to the medfate manual (https://emf-creaf. github.io/medfatebook/).

Meteorological data, including temperature (T), radiation, precipitation, and relative humidity were retrieved from historical observations from the Spanish and Catalan meteorological networks. Spatial interpolation of point data was carried out using the R package meteoland (De Cáceres et al., 2018). Model parameterization was achieved using a variety of sources, though all parameters were retrieved or calculated, and the model did not require calibration. Model validation against soil moisture and canopy transpiration measurements at several sites across the study area was performed in previous studies (De Cáceres et al. 2021, 2023; Cabon et al., 2018). Forest structure, including tree density, diameter, height and species identity were retrieved from repeated surveys carried out in 1990, 2000 and 2014 for the Spanish National Forest Inventory. Tree leaf area was then calculated based on species-specific allometric equations developed over the study area (Cabon et al., 2018) and linearly interpolated over time between each census repetition. Soil texture and rockiness were measured during the tree-core sampling campaign (Rosas et al., 2019) and species root distribution was estimated based on ecohydrological equilibrium theory, were root distribution is a function of both soil and tree properties, including leaf area and hydraulics (Cabon et al., 2018). Physiological trait parameters were obtained at the species level following the procedure from De Cáceres et al. (2023). Simulations were run for the period 1990-2015 to match meteorological, national forest inventory and tree growth data availability.

#### 2.3. Source and sink limitations to tree growth

Following the C source vs. sink limitation conceptual framework, tree growth was assumed to be under control of either or both C assimilation and cambium growth potential (i.e., the sink strength). C assimilation was simulated using medfate as the net photosynthesis (discounting leaf autotrophic respiration) per leaf area summed over a species-specific period of one year. The period end was determined for each species by optimizing the correlation between tree growth and C assimilation and extended on average from previous to current year late August, consistent with previous analyses (Cabon et al., 2022). The period end was earlier in the case of Fagus sylvatica (late July) and later in the case of Pinus halepensis (early October). In order to account for year-to-year C storage responsible for potential carry-over effects on tree growth, we also considered the role of previous year C assimilation defined as the summed annual C assimilation lagged over one year as a proxy of stored carbon (Kagawa et al., 2006; Zweifel and Sterck, 2018).

We considered the biophysical limits associated to cell turgor and

temperature constraints on cambial division as the principal driver of the sink strength. While other sink limitations, such as nutrient availability, are important drivers of tree growth, we make the assumption that their variation is negligible here, as we focus on yearly growth variability, in mature forests. Nutrients can strongly limit both photosynthesis and sink activity but, in the absence of perturbations, they vary slowly and their effect is typically expected to be gradual over time (Sullivan et al., 2014). We define the biophysical cambium potential as the potential cambial cell division rate if it were only limited by turgor-driven cell expansion and temperature-dependent cell metabolism. Based on Lockhart's (1965) equation, and assuming that cambial cells divide every time they double in size, the biophysical potential of the cambium (d) can be written as (Cabon et al., 2020b):

Biophysical potential 
$$(\Psi, T) = \begin{cases} \frac{1}{\ln 2} \cdot \phi(T) \cdot (\Psi - \Pi - \Gamma_P), \ \Psi - \Pi > \gamma_P \\ 0, \ \Psi - \Pi \leq \gamma_P \end{cases}$$
 (1)

where  $\Psi$  is the daily average tree water potential at breast height and is simulated at the plot level using medfate,  $\Pi$  is the cambium osmotic potential,  $\Gamma_P$  is the pressure yield threshold and  $\varphi$  is the cell wall extensibility. We represent the effect of temperature on the biophysical potential through variations in cell wall extensibility (Pietruszka et al., 2007), which depends upon the metabolic rate and microtubule stability dictated by temperature (Tilney and Porter, 1967; Francis and Barlow, 1988; Parent and Tardieu, 2012):

$$\phi(T) = \phi_{\text{max}} \cdot \frac{1}{1 + e^{\lambda(\Gamma_{\text{T}} - T)}} \cdot \frac{kT e^{\frac{\Delta H_{\Lambda}}{R^{\text{T}}}}}{1 - e^{\frac{\Delta S_{\text{D}}}{R^{\text{H}}}} \left(1 - \frac{\Delta H_{\text{D}}}{\Delta S_{\text{D}}}\right)}$$
(2)

Where T is the daily average plot-level air temperature,  $\varphi_{max}$  is the maximum cell wall extensibility, the second term of the equation is a sigmoid function that represents a temperature threshold of cell division, and the third term is the metabolic rate.  $\Gamma_T$  is the threshold temperature that yields the sigmoid function to equal 0.5. k and  $\lambda$  are scaling parameters,  $\Delta H_A$  is the enthalpy of activation and  $\Delta H_D$  and  $\Delta S_D$  are the enthalpy and entropy difference between the catalytically active and inactive states of the enzyme or enzymatic system.

The biophysical potential (Eq. (1)) is calculated 'offline' for each plot and species at the daily scale, using mean daily stem water potential at breast height (from medfate) and mean daily air temperature as inputs. It is parameterized at the plot level using species-specific on-site leaf measurements from Rosas et al. (2019) and  $\Gamma_p$  is calculated such that  $\Gamma_p = -0.8 \cdot \Pi$ , such as to provide meaningful results in the context of the model.  $\Gamma_T$  is set to 8°C following A Cabon et al. (2020).  $\Delta H_A$ ,  $\Delta H_D$ , and  $\Delta S_D$  are derived from previous calibration and are assumed to be the same for all plot and species (Parent et al., 2010; Parent and Tardieu, 2012). k is calculated such as  $\varphi(T_{opt}) = \varphi_{max}$ .

#### 2.4. Statistical analyses

Statistical analyses were performed to inspect modelling results. All analyses were ran for the same period than simulations (1990–2015). Because C source and sink limitations are notoriously both commonly driven by T and  $\Psi$  (Körner, 2015), we first sought to compare their response to these drivers at the daily and annual scales. Daily responses were estimated by averaging daily C assimilation and biophysical limitation across all simulations for varying values of growing season T and  $\Psi$ . To assess annual responses, we aggregated simulated photosynthesis and biophysical potential at the annual scale, and then regressed annual-scale simulations (as well as observed tree growth) against growing-season average T and  $\Psi$ . Both simulations and observations were detrended and scaled to enable comparability of estimated sensitivities. Regressions included random intercept per species and were

fitted using the R package lme4. Regression slopes were compared by means of post-hoc Tukey tests using the R package emmeans.

We further investigated C assimilation and biophysical potential covariation at the annual scale by estimating for each plot the proportion of co-variation between the respective time series, calculated as the square of Pearson's correlation coefficient (R<sup>2</sup>). The effect of climate on the amount of shared variance was then analyzed by fitting a linear model between the logit of the shared variance and plot mean annual temperature and precipitation and including a random intercept per species, again using the lme4 package.

The ability of C assimilation and biophysical potential to predict tree growth was assessed by adjusting linear models between observed plot-average, size-corrected tree growth and biophysical potential, current and previous year C assimilation, as well as first order interactions between biophysical potential and current and previous year C assimilation. One model was fitted for each plot. Goodness of fit was assessed based on the R<sup>2</sup> of the linear model and by comparing the temporal trends of observed size-corrected tree growth and simulated biophysical

limitations and C assimilation. The R<sup>2</sup> of each model was then partitioned between each factor by using the Lindeman, Merenda and Gold (LMG) metric implemented in the R package relaimpo (Grömping, 2006). Variance partition was finally analyzed on the basis of species and climate differences. The effect of climate on calculated LMG was estimated by fitting a mixed linear model (lme4 package) between logit-transformed LMG and mean annual precipitation, temperature and plot slope and including a random intercept per species.

#### 3. Results

# 3.1. Climate sensitivity and covariation of carbon assimilation and biophysical potential

Both simulated C assimilation and biophysical potential to cambium exhibited pronounced responses to  $\Psi$  and T at the daily scale. The shape of the response nevertheless strongly differed depending on the considered variable (Fig. 3A, B). Biophysical potential had a threshold

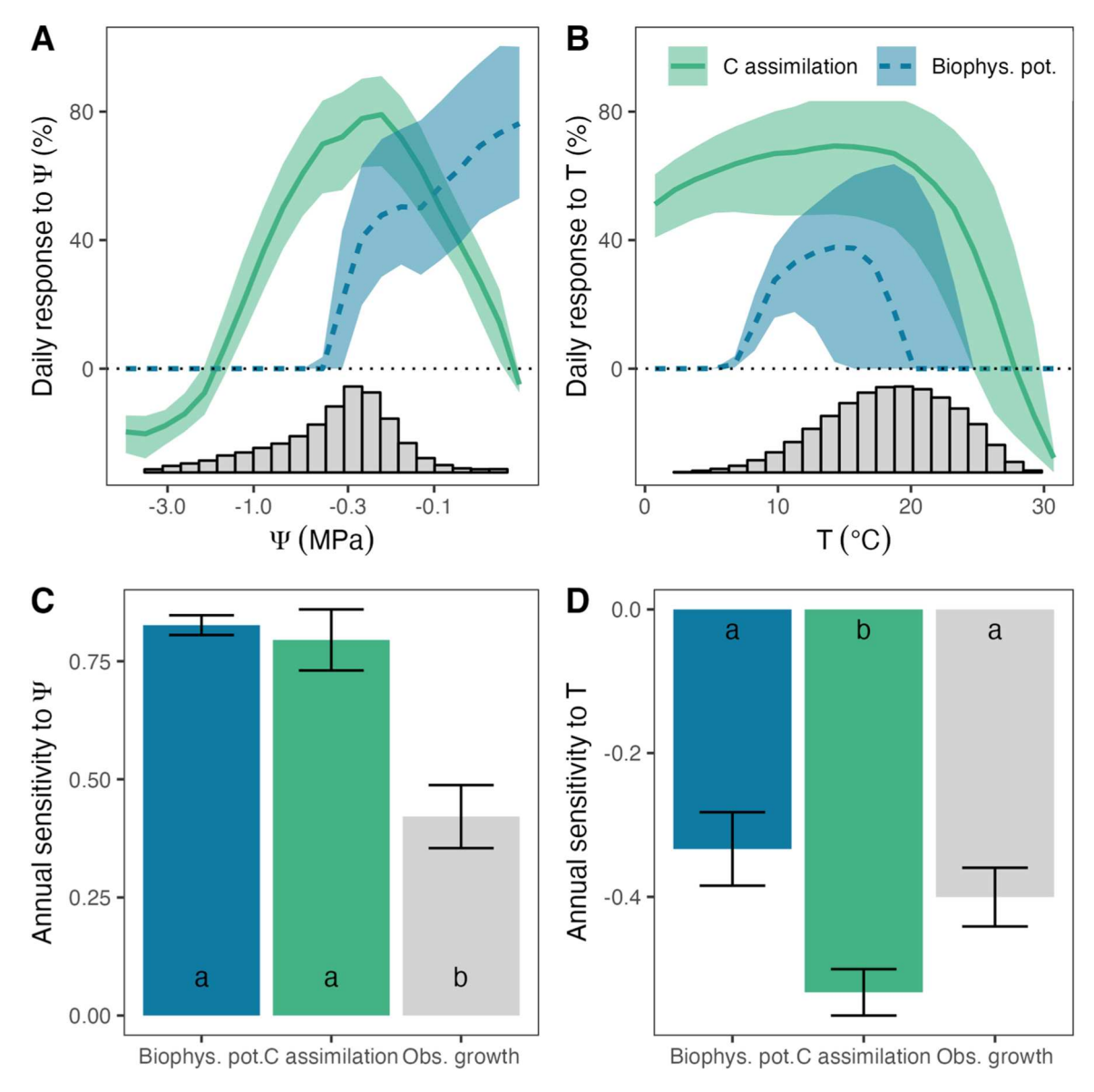


Fig. 3. Response of simulated daily C assimilation and biophysical potential to growing season (DOY 100–300) daily (A) simulated stem water potential ( $\Psi$ ) and (B) temperature (T) across all species and climatic range and over the study period (1990–2015). Lines represent averages and intervals represent the first and third quartiles. Bars show water potential and temperature distribution during the growing season. Note that a logarithmic scale is used in the x-axis of panel A. Sensitivity of annual biophysical limitations, C assimilation and observed growth to growing season average water potential (C) and temperature (D). The sensitivity was calculated as the slope of the linear relationship between the scaled response and explicative variables based on generalized linear modelling.

response to  $\Psi$  and T, with a monotonic increase above the  $\Psi$  threshold but a bell-shaped response to T, reaching zero again at high temperatures. On the other hand, T assimilation displayed a unimodal response to T with an optimum close to the point at which the biophysical function reached zero and negative response at both low and high T. C assimilation response to T was also unimodal and had similar optimum than the biophysical potential (T15°C) but T10 assimilation was much larger at low temperatures and reached negative values at high temperatures. Daily responses did not intuitively translate to the annual scale (Fig. 3C and D). Annual average T20 assimilation and biophysical potential exhibited similarly large positive sensitivity to growing season average T21, that was twice as large as that of observed growth. T22 assimilation was twice as sensitive to T32 compared to biophysical potential, which in turn compared well to observed growth sensitivity to T3.

Sensitivities of C assimilation and biophysical potential to environmental factors resulted in negative temporal trends for all species, consistent with observed size-corrected tree growth (Fig. 4). The only exceptions were Pinus sylvestris C assimilation and Fagus sylvatica biophysical potential that exhibited no significant trend. The magnitude of the trends nevertheless substantially differed across species. In the case of the three conifer species (Pinus spp.) and Quercus pubescens, biophysical limitations had a more negative trend than C assimilation, and tended to agree better with observations. On the contrary, the temporal trend of C assimilation was more negative than biophysical potential and closer to observations in the case Fagus sylvatica.

Converging sensitivity to environmental factors led annual C assimilation and biophysical potential to share a substantial proportion of their variance: about 40% on average. Covariation strongly varied between species, ranging from  ${\sim}65\%$  in the case of Pinus halepensis and  ${\sim}25\%$  in the case of Fagus sylvatica (Fig. 5A). Species differences were mostly explained by climate variations, and specifically mean annual precipitation (Fig. 5B). C assimilation and biophysical potential were more tightly linked in plots (and hence species) receiving less rainfall, with covariation ranging from  ${\sim}10\%$  (at 1200mm MAP) to over 75% (450mm MAP) along the gradient.

#### 3.2. Model performance and relative importance of explanatory variables

Taken together, C assimilation, biophysical potential and first order interactions were able to explain about 50% of observed size-corrected tree growth (Fig. 6A). Substantial plot-to-plot variations were observed but did not translate into strong differences between species. Variance decomposition of linear models of tree growth revealed

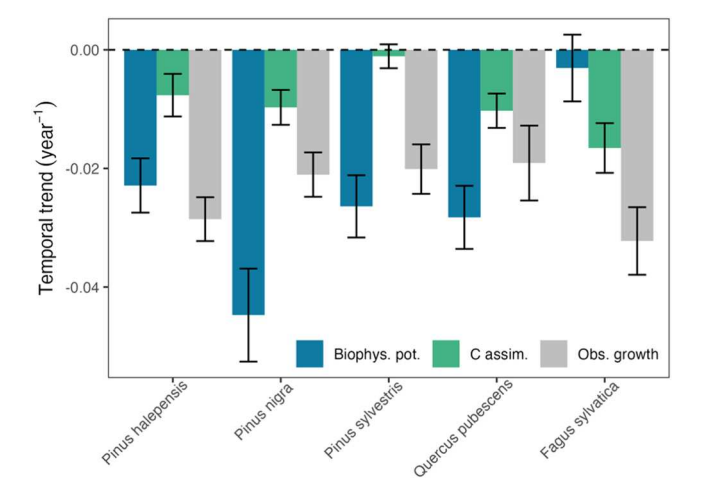


**Fig. 4.** Comparison of the slopes of temporal trends of biophysical potential, C assimilation and observed size-corrected growth. Temporal trends were calculated at the plot-level as the slope of the linear regression of each variable against time. Bars represent averages and error bars represent standard errors.

varying importance across species of biophysical and C assimilation factors to explain tree growth (Fig. 6B). Biophysical potential was in most cases the single most important variable, as it accounted for 37% of the explained variance on average, but this value varied across species from 47% (Pinus halepensis) to 16% (Fagus sylvatica). The amount of model variance that was unique to biophysical potential was somewhat stable across species (~25%). Current year C assimilation was the second most important variable, with 31% of the explained variance on average and somewhat stable across species, followed by relatively modest participation of previous year C assimilation (14%) and interactions between biophysical and photosynthetic factors (17%). Taken together C assimilation factors (both current and previous years) explained a little more variance than biophysical limitations (46% compared to 37%, respectively), but this number grew as high as 70% in the case of Fagus sylvatica.

Across species, variation in the relative importance of each factor to explain observed tree growth was related to climate (Fig. 7). Precipitation had a negative effect on the model variance explained by biophysical potential and a positive effect on that explained by previous year C assimilation, but was found to have no significant effect in the case of current year C assimilation and interactions. Overall, the amount of variance explained by biophysical factors alone strongly varied from  $\sim\!75\%$  at 450mm MAP to  $\sim\!10\%$  at 1200mm MAP, while the variance explained by previous year C assimilation varied from  $\sim\!25\%$  to  $<\!5\%$  over the same gradient. We did not find a significant effect of mean annual temperature on the proportion of explained variance of any variable.

#### 4. Discussion

#### 4.1. Converging source and sink sensitivities with aridity

Here, we report different daily responses of modelled biophysical potential and C assimilation to water potential and temperature. We observe stronger reduction of the biophysical potential compared to C assimilation at low water potential and low temperature, matching the expectation that sink activity is more strongly inhibited than source activity under these conditions (Körner, 2015). Interactions between  $\Psi$ and T led to a negative response of C assimilation and biophysical potential past an optimal temperature (15-20°C) that was sensibly lower than reported physiological optima (~30°C and above; (Parent and Tardieu, 2012; Kumarathunge et al., 2019), but somewhat consistent with ecosystem-scale optima (calculated ~23°C, from Huang et al., 2019). Relatively weak response of C assimilation to low temperature may be the result of parallel decline of temperature and radiation gross photosynthesis and leaf respiration. Decreasing C assimilation with  $\Psi >$ -0.2MPa (Fig. 3A) reflected closed stomata conditions (e.g., because of low radiation) under which minimum transpiration permits limited xylem tension. Reduced transpiration in turn provides optimal conditions for biophysical potential (Fig. 3A) (Potkay and Feng, 2023).

Despite different daily responses, we found unexpectedly similar annual sensitivity of C assimilation and biophysical potential to  $\Psi$  (Fig. 3B). This result contrasts with observed daily response differences and previous cross-biome observations (Cabon et al., 2022), as well as the expectation that biophysical potential is more sensitive to  $\Psi$  than C assimilation also at longer timescales (Muller et al., 2011). More contrasting sensitivities of biophysical potential and C assimilation to  $\Psi$  might be expected under wetter or colder climatic conditions, e.g., boreal climate, and remains to be explored. In our study region however (Mediterranean climate), generalized water limitation yielded overall large sensitivity of photosynthesis to water availability (Boisvenue and Running, 2006), which we found to further increase with aridity over the gradient.

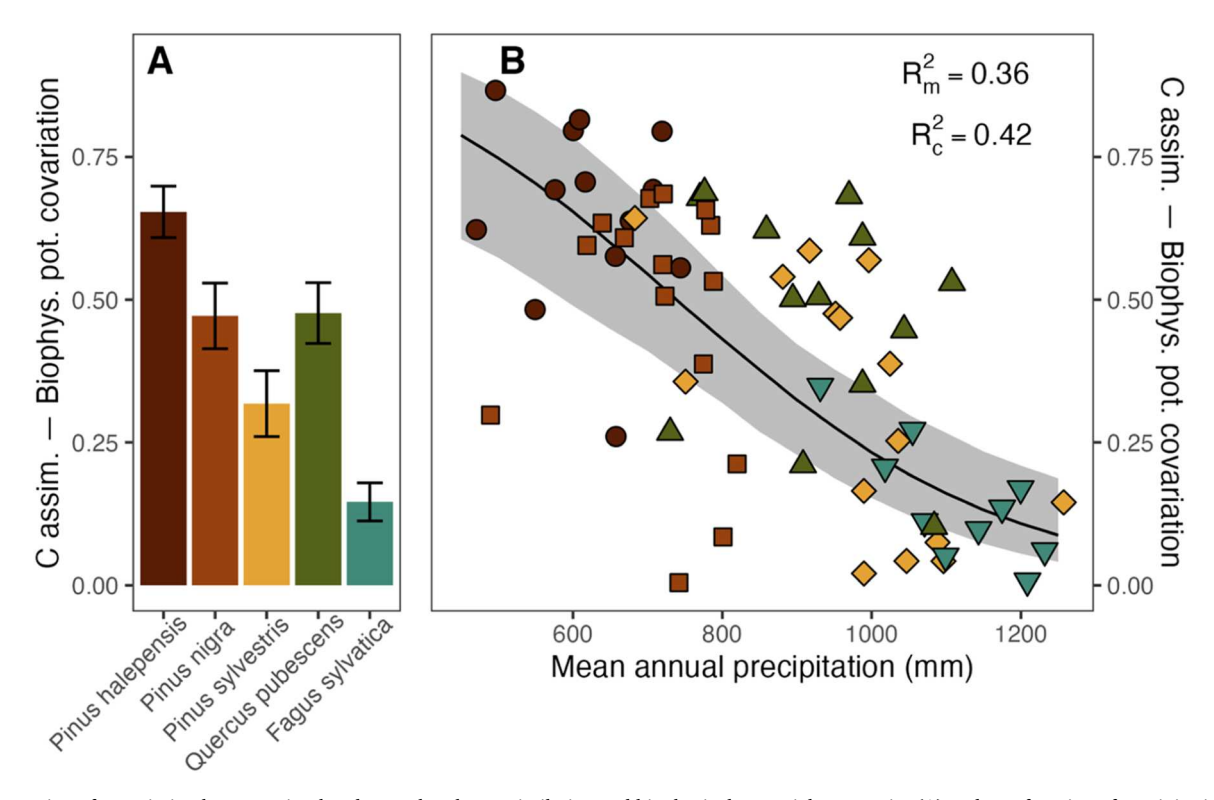
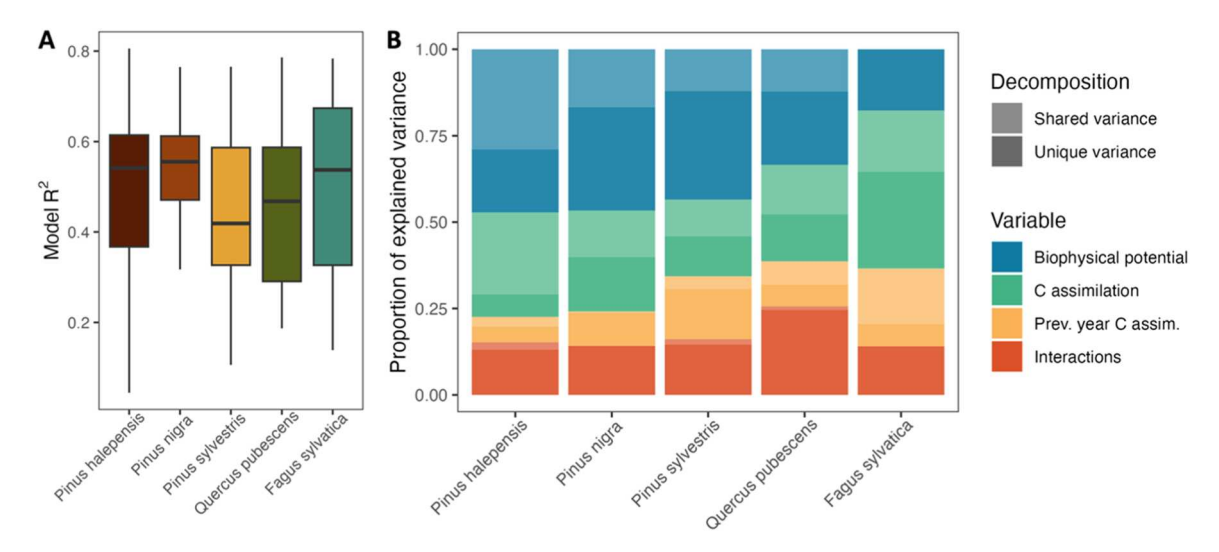


Fig. 5. Proportion of covariation between simulated annual carbon assimilation and biophysical potential per species (A) and as a function of precipitation (B). The covariation markedly increases with decreasing annual precipitation as denoted by the fitted mixed linear model (black line; 95% confidence interval represented by grey ribbon).  $R_m^2$  and  $R_c^2$  are the marginal (only fixed effects) and the conditional (both fixed and random effects)  $R^2$ , respectively. Covariation, calculated as squared Pearson correlation coefficient, was logit transformed.



**Fig. 6.** Tree growth model goodness of fit and analysis of variance. (A) Boxplot of R<sup>2</sup> of the linear models of observed tree growth against biophysical potential, C assimilation and first order interactions. Linear models were fitted individually at each plot. The lower and upper hinges correspond to the first and third quartiles. The whiskers extend from the hinges to the largest (lowest) value no further (at most) than 1.5 times the interquartile range. (B) Variance decomposition of explained growth variance per explanatory variable. Variables are represented by color hue and dark and light colors of the same hue denote unique and shared variance explained by each variable. The portion of explained growth variance accounted for by each variable was calculated as the LMG metric (Grömping, 2006), which averages the proportion of added explained variance for each variable across orderings and is thus ordering insensitive. LMG variance was further decomposed into a unique and shared portion based on type II ANOVA, where unique variance is the added model variance when adding the considered predictor on top of all the others and shared variance is the difference between LMG and unique variance. Results are species averages.

## 4.2. Increasing source-sink covariation but also sink limitation with aridity

Overall, similar annual sensitivities of simulated C assimilation and biophysical potential resulted in substantial covariation between these

processes. Covariation typically hinders disentangling C source and sink controls of tree growth (Fatichi et al., 2014), but its strength may vary with climate. Here, as a result of larger C assimilation sensitivity to  $\Psi$ , its covariation with biophysical potential strongly increased across our aridity gradient (Fig. 5). Similarly, source-sink covariation would be

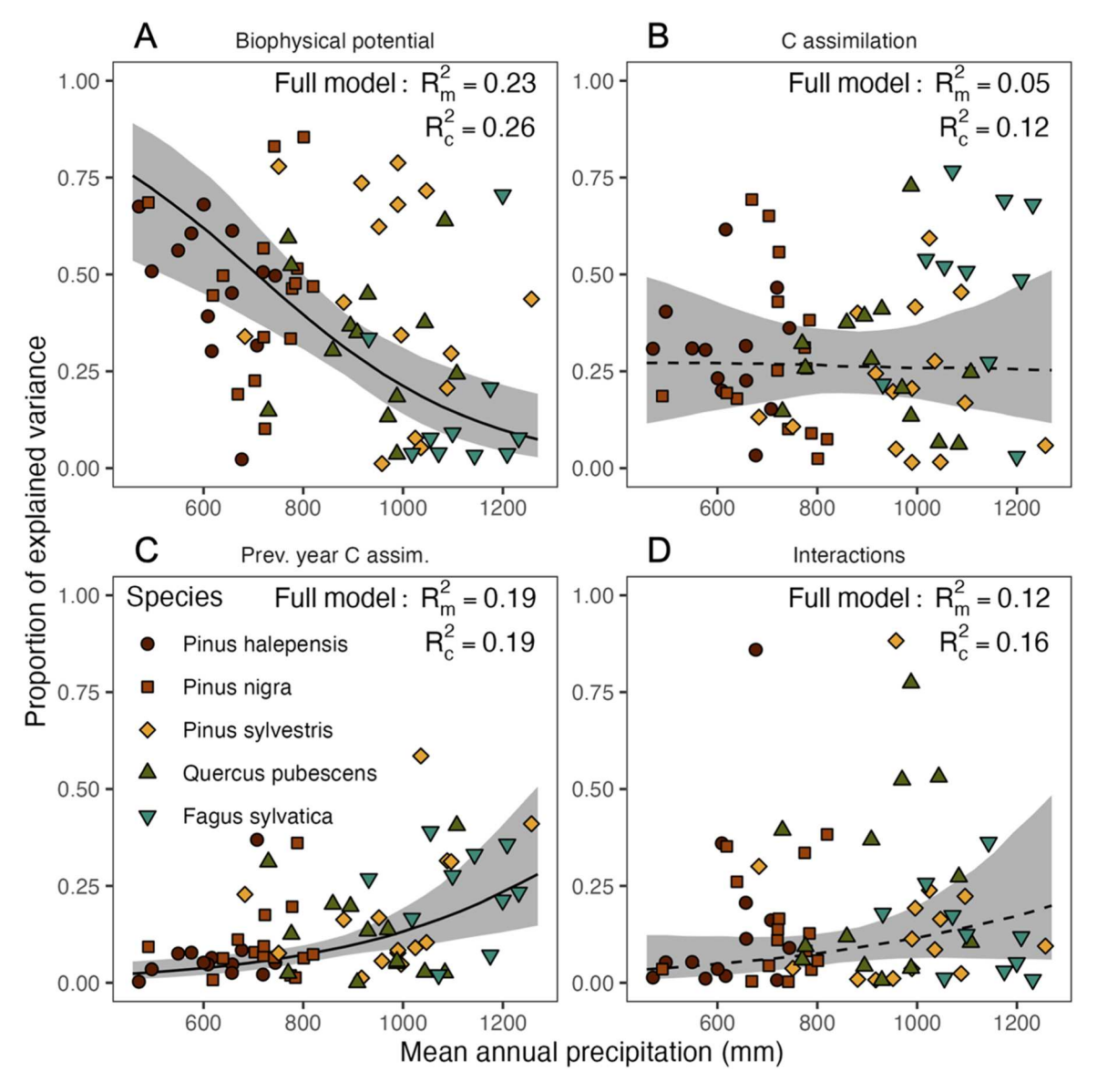


Fig. 7. Effect of climate on the amount of tree growth variance explained (LMG) by (A) biophysical limitations, (B) current year C assimilation, (C) previous year C assimilation and (D) interactions. Mixed linear models were fitted independently for each variable between logit transformed LMG vs. plot mean annual precipitation, temperature and plot slope. Models included a random intercept per species. Black lines and grey intervals represent the average and bootstrapped 95% confidence interval of the effect of precipitation on LMG, holding mean annual temperature and plot slope constant. Continuous and dashed lines represent significant and non-significant precipitation effects ( $\alpha = 0.05$ ), respectively.

expected to increase with decreasing temperature temperature-limited climate (e.g., boreal or subalpine forests). Large temporal covariation under pronounced drought (or low temperature) suggests that accounting biophysical on top of C assimilation may be redundant in these circumstances. Despite temporal covariation, we observe that simulated biophysical potential declines faster than C assimilation across species' aridity gradient (Fig. S1): biophysical potential at species' dry end averaged 20% of its maximum, against 50% in the case of C assimilation. This suggests that biophysical becomes increasingly limiting with aridity in the region. Though our study is dependent on modelling assumptions, our results agree with theoretical expectations that biophysical potential decreases faster than C assimilation with drought (Fatichi et al., 2014; Körner, 2015). Elevation gradients further provide some evidence that sink activity also becomes more limiting with cold temperatures. Namely, larger starch pools at tree lines than lower elevations counterparts, suggest excess C assimilation relative to sink activity (Shi et al., 2008; Hoch and Körner, 2012). Opposite patterns were nevertheless observed when considering variations across species and biomes (Blumstein et al., 2023), which suggests that other mechanisms might control non-structural carbon pool size at larger scales.

Our simulations show a temporal decline of both biophysical potential and C assimilation. These trends were driven by declining tree water status ( $\Psi$ ), which was the result of increasing stand density from historical rural abandonment in the region, and climate dryness (De Cáceres et al., 2015; Vayreda et al., 2016). Consistent with spatial variations, decreasing  $\Psi$  led to stronger decline of biophysical potential than C assimilation. We did not account for the fertilization effect of increased  $CO_2$  concentration on photosynthesis (Körner et al., 2007; Walker et al., 2021), which would arguably lead to less negative trends in simulated C assimilation (McDowell et al., 2022). Observed tree growth also tended to decline, at a rate that appeared in-between that of biophysical potential and C assimilation. Further drought exacerbation under climate change and  $CO_2$  fertilization are likely to lead to increasing sink limitations and more negative growth trends than would have been predicted based on C assimilation alone. Not accounting for

biophysical potential may thus lead to underestimate growth decline under increasingly dry conditions by models, including in boreal and subalpine forests (e.g., Tei et al., 2017; Mirabel et al., 2022).

#### 4.3. Source-sink decoupling

Our results show that simulated C assimilation and biophysical potential overall explained a similar share of observed tree growth variations. We nevertheless found strong variations of the relative importance of C assimilation and biophysical potential between species, which were mostly related to the degree of aridity encompassed by their distribution. As a result, temperate species (Fagus sylvatica, Pinus sylvestris) exhibited larger relative importance of carbon assimilation on growth compared to Mediterranean species (Quercus pubescens, Pinus halepensis). We note that in a previous modelling study, Fagus sylvatica growth was also observed to relate mostly to C assimilation (Guillemot et al., 2015). Our results are further consistent with evidence of decoupling between C assimilation and tree growth that tends to increase under environmental constraints (Klein et al., 2016; Jiang et al., 2020; A Cabon et al., 2022). Hence, despite drought or low temperature may lead to increasing temporal covariation between source and sink activity, a larger decrease of biophysical potential nevertheless leads to stronger sink limitations and source-sink decoupling under these conditions, consistent with emprical evidence (Lempereur et al., 2015; Thompson et al., 2023). Overall, our finding that current year C assimilation explains about ~13% of growth variance (~50% model variance  $\times$  25% of model variance attributable to current year C assimilation), is on the same order of magnitude than the 7-14% explained variance (equivalent to the 0.26–0.38 correlation in the text) reported in A Cabon et al. (2022), and strongly suggests that observed temporal decoupling between growth and photosynthesis is caused by sink limitations of tree growth, including the effect of biophysical constraints on cambial activity.

#### 4.4. Source-sink interactions

Unexpectedly, decreasing importance of biophysical potential with increasing precipitation was matched by increasing importance of previous year C assimilation, rather than current year. This result suggests that under sufficient water supply, tree growth relied increasingly upon previous year C rather than current, which is consistent with observations of larger growth autocorrelation with increasing water availability (Granda et al., 2013). Despite growth reliance on current year C could not be explained based on climate variables, it nevertheless varied widely between sites. This variation was in part related to cross-species differences (half of the model variance is explained by the random species effect in Fig. 7B), hinting that source limitation might in part be driven by species traits (e.g., deciduousness, photosynthetic capacity). Varying effect of C assimilation on tree growth was also illustrated, over time, by negative multiplicative interactions with biophysical potential in two out of five species (Fig. S2). Negative interactions implied lower biophysical constraints on tree growth under ample C assimilation activity and reciprocally. This suggests that C availability helps mitigating sink limitation through some compensation mechanism, e.g., osmotic regulation, a key process of drought acclimation that requires substantial C inputs (Woodruff and Meinzer, 2011; Bartlett et al., 2014).

#### 4.5. Implications for tree growth modelling

Here we show that simulated C assimilation and biophysical potential allowed to predict about half of observed temporal (annual and decadal) variations in tree radial growth. As 28% of the variance in our tree growth series is actually noise (average expressed population signal = 0.72), we estimate that our statistical model was able to explain about two thirds of signal variance. Despite large covariation, adding a biophysical potential term in addition to C assimilation noticeably

improved model fit (as denoted added by explained variance and  $\Delta$ AIC, Fig. 6, Table S2), providing additional evidence to the relevance of accounting for sink limitations to model tree growth and its temporal variations, especially toward the dry end of our gradient (Guillemot et al., 2015; Schiestl-Aalto et al., 2015). Additionally, the non-neglectable role of previous year C assimilation on tree growth, especially toward the wet end of our gradient, advocates for the consideration of C storage in models (e.g., Jones et al., 2019).

Although there is growing consensus on the need to integrate sink limitations to vegetation models, such as DGVMs, the question remains of how to implement it in practice. Building up on dynamic allocation coefficients implemented in some in DGVMs, by having allocation coefficient representing sink limitation, is a relatively straightforward solution (Guillemot et al., 2015, 2017; Fatichi et al., 2019). Such an approach nevertheless makes the underlying assumption that the effect of source and sink limitations on tree growth is multiplicative and positive. An alternative formulation, is that source-sink interactions follow Liebig's law of minimum (Fatichi et al., 2014), which in first approximation resembles positive multiplicative interaction in a linear framework. The finding that biophysical potential drives tree growth when more limiting than photosynthesis (dry end of our climate gradient) is partial evidence of positive multiplicative interactions across space, qualitatively analogous to Liebig's law. However, linear modelling of temporal growth variations suggests that, over time, source-sink interactions are instead mostly additive with limited negative multiplicative interactions. This result is consistent with observed temporal response of tree growth to past volcanic eruptions (Cabon and Anderegg, 2023). Hence, interactions between photosynthesis and biophysical potential appear to differ across space and time. The biophysical potential framework can accomodate both multiplicative and additive interactions. For example, assuming that temporal adjustment of osmotic potential in response to drought (Bartlett et al., 2014), which requires sugars amongst other osmolytes, is under control of C assimilation would indeed result in an additive effect of water potential and C assimilation in Eq. (1) (Potkay and Feng, 2023). On the other hand, the number of cells able to divide in the cambium, which product with the cell division rate yields total cell production, varies between individuals, likely in relation to trees' photosynthetic capacity (Vaganov et al., 2006). An effect of photosynthetic capacity on cambial cell number would thus be consistent with multiplicative interactions source-sink across space suggested here, but more evidence is required to test this hypothesis.

#### 5. Conclusion

Overall, we provide evidence that accounting for biophysical limitations on top of C assimilation holds potential to represent sink limitations to tree growth and improve tree growth modelling. We further evidence patterns of variations of source and sink limitations, which suggest that source-sink interactions are mostly additive over time but may be multiplicative across space (Liebig's law analogy). More research is needed to clarify these patterns, which models will need to replicate. By scaling up Lockhart's equation to the tree level, the biophysical potential framework represents a good candidate to integrate source and sink limitations and has the potential to accommodate additive and multiplicative interactions. Observations of Lockhart's equation terms in trees growing in natural conditions are scarce (e.g., Woodruff and Meinzer, 2011), but understanding how they vary, notably in response source dynamics, will help moving forward in characterizing the mechanisms underlying source-sink interactions and their implementation in models.

#### CRediT authorship contribution statement

**Antoine Cabon:** Conceptualization, Methodology, Formal analysis, Data curation, Writing – original draft, Writing – review & editing,

Visualization. Aitor Ameztegui: Methodology, Writing – review & editing. William R.L. Anderegg: Writing – review & editing, Supervision, Funding acquisition. Jordi Martínez-Vilalta: Conceptualization, Writing – review & editing, Supervision, Funding acquisition. Miquel De Cáceres: Conceptualization, Methodology, Writing – review & editing, Supervision, Funding acquisition.

#### **Declaration of Competing Interest**

The authors declare that they have no known competing financial interests or personal relationships that could have appeared to influence the work reported in this paper.

#### Data availability

Data will be made available on request.

#### Acknowledgments

AC and WA acknowledge funding from USDA National Institute of Food and Agriculture, Agricultural and Food Research Initiative Competitive Programme, Ecosystem Services and Agro-Ecosystem Management, grant no. 2018–67019–27850. AC also acknowledges support from the Swiss National Science Foundation through the project MiCSS (TMPFP3–209811). AA obtained a Serra-Húnter fellowship from Generalitat de Catalunya. WA is supported by the David and Lucille Packard Foundation and US National Science Foundation grants no. 1714972, 1802880, 2044937, and 2003017. JM-V benefited from an ICREA Academia award. MdC acknowledges support from project BOMFORES (project no. PID2021–1266790B-I00 funded by MCIN/AEI /10.13039/501100011033 and the European Union's Next Generation EU/ PRTR). Empirical data was obtained thanks to grant CGL2013–46808-R, funded by the Spanish Ministry of Science and Innovation.

#### Supplementary materials

Supplementary material associated with this article can be found, in the online version, at doi:10.1016/j.agrformet.2023.109852.

#### References

- Bartlett, M.K., Zhang, Y., Kreidler, N., Sun, S., Ardy, R., Cao, K., Sack, L., 2014. Global analysis of plasticity in turgor loss point, a key drought tolerance trait. Ecol. Lett. 17, 1580–1590.
- Blumstein, M., Gersony, J., Martínez-Vilalta, J., Sala, A., 2023. Global variation in nonstructural carbohydrate stores in response to climate. Glob. Change Biol. 29, 1854–1869.
- Boisvenue, C., Running, S.W., 2006. Impacts of climate change on natural forest productivity evidence since the middle of the 20th century. Glob. Change Biol. 12, 862–882.
- Bonan, G.B., 2008. Forests and climate change: forcings, feedbacks, and the climate benefits of forests. Science 320, 1444–1449.
- Cabon, A., Anderegg, W.R.L., 2022. Turgor-driven tree growth: scaling-up sink limitations from the cell to the forest (S Sevanto, Ed.). Tree Physiol. 42, 225–228.
- Cabon, A., Anderegg, W.R.L., 2023. Large volcanic eruptions elucidate physiological controls of tree growth and photosynthesis. Ecol. Lett. 26, 257–267.
- Cabon, A., Fernández-de-Uña, L., Gea-Izquierdo, G., Meinzer, F.C., Woodruff, D.R., Martínez-Vilalta, J., De Cáceres, M., 2020a. Water potential control of turgor-driven tracheid enlargement in Scots pine at its xeric distribution edge. New Phytol. 225, 209–221.
- Cabon, A., Kannenberg, S.A., Arain, A., Babst, F., Baldocchi, D., Belmecheri, S., Delpierre, N., Guerrieri, R., Maxwell, J.T., McKenzie, S., et al., 2022. Cross-biome synthesis of source versus sink limits to tree growth. Science 376, 758–761.
- Cabon, A., Martínez-Vilalta, J., Martínez de Aragón, J., Poyatos, R., De Cáceres, M, 2018. Applying the eco-hydrological equilibrium hypothesis to model root distribution in water-limited forests. Ecohydrology 11, e2015.
- Cabon, A., Peters, R.L., Fonti, P., Martínez-Vilalta, J., De Cáceres, M., 2020b. Temperature and water potential co-limit stem cambial activity along a steep elevational gradient. New Phytol. 226, 1325–1340.
- De Cáceres, M., Martínez-Vilalta, J., Coll, L., Llorens, P., Casals, P., Poyatos, R., Pausas, J. G., Brotons, L., 2015. Coupling a water balance model with forest inventory data to

- predict drought stress: the role of forest structural changes vs. climate changes. Agric. For. Meteorol. 213, 77–90.
- De Cáceres, M., Martin-StPaul, N., Turco, M., Cabon, A., Granda, V., 2018. Estimating daily meteorological data and downscaling climate models over landscapes. Environ. Model. Softw. 108, 186–196.
- De Cáceres, M., Mencuccini, M., Martin-StPaul, N., Limousin, J.M., Coll, L., Poyatos, R., Cabon, A., Granda, V., Forner, A., Valladares, F., et al., 2021. Unravelling the effect of species mixing on water use and drought stress in Mediterranean forests: a modelling approach. Agric. For. Meteorol. 296, 108233.
- Cartenì, F., Deslauriers, A., Rossi, S., Morin, H., De Micco, V., Mazzoleni, S., Giannino, F., 2018. The physiological mechanisms behind the earlywood-to-latewood transition: a process-based modeling approach. Front. Plant Sci. 9, 1–12.
- Collatz, G.J., Ball, J.T., Grivet, C., Berry, J.A., 1991. Physiological and environmental regulation of stomatal conductance, photosynthesis and transpiration: a model that includes a laminar boundary layer. Agric. For. Meteorol. 54, 107–136.
- Collins, M., Chandler, R.E., Cox, P.M., Huthnance, J.M., Rougier, J., Stephenson, D.B., 2012. Quantifying future climate change. Nat. Clim. Change 2, 403–409.
- Cook, E.R., Kairiukstis, L.A., 2013. Methods of Dendrochronology: Applications in the Environmental Sciences. Springer Science & Business Media.
- Coussement, J.R., De Swaef, T., Lootens, P., Roldán-Ruiz, I., Steppe, K., 2018.
  Introducing turgor-driven growth dynamics into functional-structural plant models.
  Ann. Bot. 121, 849–861.
- De Cáceres, M., Molowny-Horas, R., Cabon, A., Martínez-Vilalta, J., Mencuccini, M., García-Valdés, R., Nadal-Sala, D., Sabaté, S., Martin-StPaul, N., Morin, X., et al., 2023. MEDFATE 2.9.3: a trait-enabled model to simulate Mediterranean forest function and dynamics at regional scales. Geosci. Model. Dev. 16, 3165–3201.
- Deslauriers, A., Giovannelli, A., Rossi, S., Castro, G., Fragnelli, G., Traversi, L., 2009. Intra-annual cambial activity and carbon availability in stem of poplar. Tree Physiol. 29, 1223–1235.
- Deslauriers, A., Huang, J.G., Balducci, L., Beaulieu, M., Rossi, S., 2016. The contribution of carbon and water in modulating wood formation in black spruce saplings. Plant Physiol. 170, 2072–2084.
- Fatichi, S., Leuzinger, S., Körner, C., 2014. Moving beyond photosynthesis: from carbon source to sink-driven vegetation modeling. New Phytol. 201, 1086–1095.
- Fatichi, S., Pappas, C., Zscheischler, J., Leuzinger, S., 2019. Modelling carbon sources and sinks in terrestrial vegetation. New Phytol. 221, 652–668.
- Fisher, R.A., Koven, C.D., Anderegg, W.R.L., Christoffersen, B.O., Dietze, M.C., Farrior, C. E., Holm, J.A., Hurtt, G.C., Knox, R.G., Lawrence, P.J., et al., 2018. Vegetation demographics in earth system models: a review of progress and priorities. Glob. Change Biol. 24, 35–54.
- Francis, D., Barlow, P.W., 1988. Temperature and the cell cycle. Symp. Soc. Exp. Biol. 42, 181–201.
- Franklin, O., Johansson, J., Dewar, R.C., Dieckmann, U., McMurtrie, R.E., Brännström, A. K., Dybzinski, R., 2012. Modeling carbon allocation in trees: a search for principles. Tree Physiol. 32, 648–666.
- Friedlingstein, P., O'Sullivan, M., Jones, M.W., Andrew, R.M., Gregor, L., Hauck, J., Le Quéré, C., Luijkx, I.T., Olsen, A., Peters, G.P., et al., 2022. Global Carbon Budget 2022. Earth Syst. Sci. Data 14, 4811–4900.
- Friend, A.D., Eckes-Shephard, A.H., Fonti, P., Rademacher, T.T., Rathgeber, C.B.K., Richardson, A.D., Turton, R.H., 2019. On the need to consider wood formation processes in global vegetation models and a suggested approach. Ann. For. Sci. 76, 49.
- Friend, A.D., Lucht, W., Rademacher, T.T., Keribin, R., Betts, R., Cadule, P., Ciais, P., Clark, D.B., Dankers, R., Falloon, P.D., et al., 2014. Carbon residence time dominates uncertainty in terrestrial vegetation responses to future climate and atmospheric CO2. Proc. Natl. Acad. Sci. U. S. A. 111, 3280–3285.
- Gómez-Aparicio, L., García-Valdés, R., Ruíz-Benito, P., Zavala, M.A., 2011. Disentangling the relative importance of climate, size and competition on tree growth in Iberian forests: implications for forest management under global change. Glob. Change Biol. 17, 2400–2414.
- González de Andrés, E., Rosas, T., Camarero, J.J., Martínez-Vilalta, J., 2021. The intraspecific variation of functional traits modulates drought resilience of European beech and pubescent oak. J. Ecol. 109, 3652–3669.
- Granda, E., Camarero, J.J., Gimeno, T.E., Martínez-Fernández, J., Valladares, F., 2013. Intensity and timing of warming and drought differentially affect growth patterns of co-occurring Mediterranean tree species. Eur. J. For. Res. 132, 469–480.
- Grömping, U., 2006. Relative importance for linear regression in R: the package relaimpo. J. Stat. Softw. 17, 1–27.
- Guillemot, J., Francois, C., Hmimina, G., Dufrêne, E., Martin-StPaul, N.K., Soudani, K., Marie, G., Ourcival, J.M.M., Delpierre, N, 2017. Environmental control of carbon allocation matters for modelling forest growth. New Phytol. 214, 180–193.
- Guillemot, J., Martin-StPaul, N.K., Dufréne, E., François, C., Soudani, K., Ourcival, J.M., Delpierre, N., 2015. The dynamic of the annual carbon allocation to wood in European tree species is consistent with a combined source–sink limitation of growth: implications for modelling. Biogeosciences 12, 2773–2790.
- Hoch, G., Körner, C., 2012. Global patterns of mobile carbon stores in trees at the highelevation tree line. Glob. Ecol. Biogeogr. 21, 861–871.
- Hölttä, T., Mäkinen, H., Nöjd, P., Mäkelä, A., Nikinmaa, E., 2010. A physiological model of softwood cambial growth. Tree Physiol. 30, 1235–1252.
- Hsiao, T.C., 1973. Plant responses to water stress. Annu. Rev. Plant Biol. 24, 519–570.
  Huang, M., Piao, S., Ciais, P., Peñuelas, J., Wang, X., Keenan, T.F., Peng, S., Berry, J.A.,
  Wang, K., Mao, J., et al., 2019. Air temperature optima of vegetation productivity across global biomes. Nat. Ecol. Evol. 3, 772–779.
- Jiang, M., Medlyn, B.E., Drake, J.E., Duursma, R.A., IC, Anderson, Barton, C.V.M., Boer, M.M., Carrillo, Y., Castañeda-Gómez, L., Collins, L., et al., 2020. The fate of carbon in a mature forest under carbon dioxide enrichment. Nature 580, 227–231.

- Jones, S., Rowland, L., Cox, P., Hemming, D., Wiltshire, A., Williams, K., Parazoo, N., Liu, J., da Costa, A., Meir, P., et al., 2019. The impact of a simple representation of non-structural carbohydrates on the simulated response of tropical forests to drought. Biogeosciences Discuss. 1–26.
- Kagawa, A., Sugimoto, A., Maximov, T.C., 2006. Seasonal course of translocation, storage and remobilization of <sup>13</sup>C pulse-labeled photoassimilate in naturally growing Larix gmelinii saplings. New Phytol. 171, 793–804.
- Klein, T., Bader, M.K.F., Leuzinger, S., Mildner, M., Schleppi, P., Siegwolf, R.T.W., Körner, C., 2016. Growth and carbon relations of mature Picea abies trees under 5 years of free-air CO2 enrichment. J. Ecol. 104, 1720–1733.
- Körner, C., 2015. Paradigm shift in plant growth control. Curr. Opin. Plant Biol. 25, 107–114
- Körner, C., Morgan, J., Norby, R., 2007. CO2 fertilization: when, where, how much? Canadell JG, Pataki DE, Pitelka LF Terrestrial Ecosystems in a Changing World. Springer Berlin Heidelberg, Berlin, Heidelberg, pp. 9–21.
- Kumarathunge, D.P., Medlyn, B.E., Drake, J.E., Tjoelker, M.G., Aspinwall, M.J., Battaglia, M., Cano, F.J., Carter, K.R., Cavaleri, M.A., Cernusak, L.A., et al., 2019. Acclimation and adaptation components of the temperature dependence of plant photosynthesis at the global scale. New Phytol. 222, 768–784.
- Lempereur, M., Martin-StPaul, N.K., Damesin, C., Joffre, R., Ourcival, J., Rocheteau, A., Rambal, S., 2015. Growth duration is a better predictor of stem increment than carbon supply in a Mediterranean oak forest: implications for assessing forest productivity under climate change. New Phytol. 207, 579–590.
- Lockhart, J.A., 1965. An analysis of irreversible plant cell elongation. J. Theor. Biol. 8, 264-275
- McDowell, N.G., Sapes, G., Pivovaroff, A., Adams, H.D., Allen, C.D., Anderegg, W.R.L., Arend, M., Breshears, D.D., Brodribb, T., Choat, B., et al., 2022. Mechanisms of woody-plant mortality under rising drought, CO2 and vapour pressure deficit. Nat. Rev. Earth Environ. 3, 294–308.
- Medlyn B.E., Loustau D., Delzon S. 2002. Temperature response of parameters of a biochemically based model of photosynthesis. I. Seasonal changes in mature maritime pine (Pinus pinaster Ait.). Plant Cell Environ. 25: 1155–1165.
- Merganičová, K., Merganič, J., Lehtonen, A., Vacchiano, G., Sever, M.Z.O., Augustynczik, A.L.D., Grote, R., Kyselová, I., Mäkelä, A., Yousefpour, R., et al., 2019. Forest carbon allocation modelling under climate change. Tree Physiol. 39, 1937–1960.
- Mirabel, A., Girardin, M.P., Metsaranta, J., Campbell, E.M., Arsenault, A., Reich, P.B., Way, D., 2022. New tree-ring data from Canadian boreal and hemi-boreal forests provide insight for improving the climate sensitivity of terrestrial biosphere models. Sci. Total Environ. 851, 158062.
- Muller, B., Pantin, F., Génard, M., Turc, O., Freixes, S., Piques, M., Gibon, Y., 2011. Water deficits uncouple growth from photosynthesis, increase C content, and modify the relationships between C and growth in sink organs. J. Exp. Bot. 62, 1715–1729.
- Pan, Y., Birdsey, R.A., Fang, J., Houghton, R., Kauppi, P.E., Kurz, W.A., Phillips, O.L., Shvidenko, A., Lewis, S.L., Canadell, J.G., et al., 2011. A large and persistent carbon sink in the world's forests. Science 333, 988–993.
- Pappas, C., Fatichi, S., Leuzinger, S., Wolf, A., Burlando, P., 2013. Sensitivity analysis of a process-based ecosystem model: pinpointing parameterization and structural issues. J. Geophys. Res. Biogeosciences 118, 505–528.
- Parent, B., Tardieu, F., 2012. Temperature responses of developmental processes have not been affected by breeding in different ecological areas for 17 crop species. New Phytol. 194, 760–774.
- Parent, B., Turc, O., Gibon, Y., Stitt, M., Tardieu, F., 2010. Modelling temperature-compensated physiological rates, based on the co-ordination of responses to temperature of developmental processes. J. Exp. Bot. 61, 2057–2069.
- Peters, R.L., Steppe, K., Cuny, H.E., De Pauw, D.J.W., Frank, D.C., Schaub, M., Rathgeber, C.B.K., Cabon, A., Fonti, P., 2021. Turgor – a limiting factor for radial growth in mature conifers along an elevational gradient. New Phytol. 229, 213–229.
- Pietruszka, M., Lewicka, S., Pazurkiewicz-Kocot, K., 2007. Temperature and the growth of plant cells. J. Plant Growth Regul. 26, 15–25.
- Piper, F.I., Fajardo, A., Hoch, G., 2017. Single-provenance mature conifers show higher non-structural carbohydrate storage and reduced growth in a drier location. Tree Physiol. 37, 1001–1010.
- Potkay, A., Feng, X., 2023. Do stomata optimize turgor-driven growth? A new framework for integrating stomata response with whole-plant hydraulics and carbon balance. New Phytol. 238, 506–528.

- Potkay, A., Hölttä, T., Trugman, A.T., Fan, Y., 2022. Turgor-limited predictions of tree growth, height and metabolic scaling over tree lifespans (M Ryan, Ed.). Tree Physiol. 42, 229–252.
- Pugh, T.A.M., Rademacher, T., Shafer, S.L., Steinkamp, J., Barichivich, J., Beckage, B., Haverd, V., Harper, A., Heinke, J., Nishina, K., et al., 2020. Understanding the uncertainty in global forest carbon turnover. Biogeosciences 17, 3961–3989.
- Quillet, A., Peng, C., Garneau, M., 2010. Toward dynamic global vegetation models for simulating vegetation-climate interactions and feedbacks: recent developments, limitations, and future challenges. Environ. Rev. 18, 333–353.
- Rosas, T., Martínez-Vilalta, J., Mencuccini, M., Cochard, H., Barba, J., Saura-Mas, S., Cochard, H., Saura-Mas, S., Martínez-Vilalta, J., 2019. Adjustments and coordination of hydraulic, leaf and stem traits along a water availability gradient. New Phytol. 223. 632-646.
- Rossi, S., Deslauriers, A., Griçar, J., Seo, J.W., Rathgeber, C.B.K., Anfodillo, T., Morin, H., Levanic, T., Oven, P., Jalkanen, R., 2008. Critical temperatures for xylogenesis in conifers of cold climates. Glob. Ecol. Biogeogr. 17, 696–707.
- Schiestl-Aalto, P., Kulmala, L., Harri, M., Mäkinen, H., Nikinmaa, E., Mäkelä, A., 2015. CASSIA - a dynamic model for predicting intra-annual sink demand and interannual growth variation in Scots pine. New Phytol. 206, 647–659.
- Serra-Maluquer, X., Mencuccini, M., Martínez-Vilalta, J., 2018. Changes in tree resistance, recovery and resilience across three successive extreme droughts in the northeast Iberian Peninsula. Oecologia 187, 343–354.
- Shi, P., Körner, C., Hoch, G., 2008. A test of the growth-limitation theory for alpine tree line formation in evergreen and deciduous taxa of the eastern Himalayas. Funct. Ecol. 22, 213–220.
- Smith, R.L., Tebaldi, C., Nychka, D., Mearns, L.O., 2009. Bayesian modeling of uncertainty in ensembles of climate Models. J. Am. Stat. Assoc. 104, 97–116.
- Sperry, J.S., Venturas, M.D., Anderegg, W.R.L., Mencuccini, M., Mackay, D.S., Wang, Y., Love, D.M., 2017. Predicting stomatal responses to the environment from the optimization of photosynthetic gain and hydraulic cost. Plant Cell Environ. 40, 816–830
- Steppe, K., De Pauw, D.J.W., Lemeur, R., Vanrolleghem, P.A., 2006. A mathematical model linking tree sap flow dynamics to daily stem diameter fluctuations and radial stem growth. Tree Physiol. 26, 257–273.
- Sullivan, B.W., Alvarez-Clare, S., Castle, S.C., Porder, S., Reed, S.C., Schreeg, L., Townsend, A.R., Cleveland, C.C., 2014. Assessing nutrient limitation in complex forested ecosystems: alternatives to large-scale fertilization experiments. Ecology 95, 668-681
- Tei, S., Sugimoto, A., Yonenobu, H., Matsuura, Y., Osawa, A., Sato, H., Fujinuma, J., Maximov, T., 2017. Tree-ring analysis and modeling approaches yield contrary response of circumboreal forest productivity to climate change. Glob. Change Biol. 23, 5179–5188.
- Thompson, R.A., Adams, H.D., Breshears, D.D., Collines, A.D., Dickman, L.T., Grossiord, C., Manrique-Alba, A., Peltier, D.M., Ryan, M.G., Trowbridge, A.M., McDowell, N.G., 2023. No carbon storage in growth-limited trees in a semi-arid woodland. Nat. Commun. 14, 1959.
- Tilney, L.G., Porter, K.R., 1967. Studies on the microtubules in heliozoa. J. Cell Biol. 34, 327–343.
- Vaganov, E.A., Hughes, M.K., Shashkin, A.V., 2006. Seasonal cambium activity and production of new xylem cells. In: Growth dynamics of conifer tree rings. Springer-Verlag, Berlin/Heidelberg, pp. 71–103.
- Vayreda, J., Martinez-Vilalta, J., Gracia, M., Canadell, J.G., Retana, J., 2016.
  Anthropogenic-driven rapid shifts in tree distribution lead to increased dominance of broadleaf species. Glob. Change Biol. 22, 3984–3995.
- Walker, A.P., De Kauwe, M.G., Bastos, A., Belmecheri, S., Georgiou, K., Keeling, R.F., McMahon, S.M., Medlyn, B.E., Moore, D.J.P.P., Norby, R.J., et al., 2021. Integrating the evidence for a terrestrial carbon sink caused by increasing atmospheric CO2. New Phytol. 229, 2413–2445.
- Winkler, A., Oberhuber, W., 2017. Cambial response of Norway spruce to modified carbon availability by phloem girdling. Tree Physiol. 37, 1527–1535.
- Woodruff, D.R., Meinzer, F.C., 2011. Water stress, shoot growth and storage of nonstructural carbohydrates along a tree height gradient in a tall conifer. Plant Cell Environ. 34, 1920–1930.
- Zweifel, R., Sterck, F., 2018. A conceptual tree model explaining legacy effects on stem growth. Front. For. Glob. Change 1, 1–9.